AEROSOL TURBIDITY DERIVATION FROM BROADBAND IRRADIANCE MEASUREMENTS: METHODOLOGICAL ADVANCES AND UNCERTAINTY ANALYSIS

Christian A. Gueymard
Solar Consulting Services
P.O. Box 392
Colebrook, NH 03576
Chris@SolarConsultingServices.com

ABSTRACT

The goal of this investigation is to provide an efficient method to derive aerosol optical depth (AOD) information from conventional broadband direct normal irradiance (DNI) measurements. A critical analysis of all the difficulties associated with this method is presented. The main issues are the quality of the DNI measurements, the accurate determination of precipitable water (PW), the elimination of cloud-contaminated results, and the estimation of the Ångström exponent to evaluate the spectral AOD from the broadband AOD (BAOD). Original solutions are presented to alleviate all these issues. A performance assessment of various candidate radiative models is undertaken using radiometric and sunphotometric data at two sites. Various difficulties are identified in the implementation of the method. The uncertainty in BAOD retrieved with the best model (REST2) can be lower than ≈0.012 on a monthly basis. Although the method is intended to be of general application, its current implementation targets areas of low AOD, such as the southwest US, where many radiometric stations exist.

1. INTRODUCTION

Aerosol turbidity is an essential atmospheric variable, which conditions the magnitude and variability of solar radiation (e.g., [1]). This is particularly the case for direct normal irradiance (DNI) under conditions of low cloudiness. For increased accuracy in solar resource data, it is important to study the spatial and temporal variability of aerosols, and to improve the accuracy of solar radiation modeling over regions of critical interest for the solar industry. Atmospheric turbidity is normally measured by the aerosol optical depth (AOD) at some key wavelengths. For the last two decades, AOD has been accurately observed with ground-based multiwavelength sunphotometers, such as those belonging to the AERONET network. However, the number of such stations is insufficient over most world areas, particularly those of interest for solar power production, like the southwest US. Because of the large spatial and temporal variability of aerosols, interpolating between AERONET sites is usually not conducive of accurate AOD determinations. Other sources of AOD information exist, particularly those based on

spaceborne observations, from, e.g., the MODIS instrument. However, such data may be far from accurate over regions of low turbidity and highly-reflective ground, such as the southwest US [2]. To increase the spatial coverage of AOD observations over areas of high potential interest for solar power, it is desirable to use other sources of data.

In this context, the goal of this study is to obtain reliable estimates of AOD in areas where only broadband radiometric stations are deployed that include measurements of DNI. The number of such stations has increased significantly in recent years because of the need for reliable solar resource assessment data to accelerate the development of solar power. Some of these stations have been supported by NREL in the framework of the SOLRMAP project [3, 4]. The value of such radiometric measurements can be enhanced dramatically if one can extract aerosol information from them. NREL's current applications (such as the National Solar Radiation Data Base, NSRDB) use AOD information based on climatological means with a monthly temporal resolution. A method capable of delivering reliable time series of AOD information at that time scale (or finer) is at the core of this project.

The idea of deriving aerosol information from irradiance measurements is not new, since it can be traced back to the very concept of the Linke turbidity factor, introduced in 1922. The Unsworth-Monteith turbidity coefficient, or "broadband aerosol optical depth" was introduced 50 years later. This coefficient, τ_a, is only marginally dependent on precipitable water, PW, and air mass [5], and was selected by NREL to develop the original NSRDB. It was then derived using hourly DNI data (under assumed cloudless conditions) and the METSTAT model [6, 7] used backwards. A similar technique, but aimed at producing the Ångström turbidity coefficient, β, was proposed by Louche et al. [8]. Various authors independently proposed similar techniques, as reviewed in [5]. The latter contribution also proposed an elaborate method to derive both τ_a and β from DNI data at high temporal resolution. To obtain β from τ_a, the method used the conventional fixed value of 1.3 for the Ångström exponent, α, which describes how the spectral AOD varies with wavelength according to Ångström's Law.

This contribution examines the performance of various possible models that can derive aerosol information from DNI data, as well as the sources of uncertainty in the final results. Five critical issues are examined in detail: (i) instrument error; (ii) impact of model performance; (iii) propagation of errors due to incorrect PW; (iv) elimination of cloudy conditions; and (v) evaluation of α. A validation of the method, using collocated radiometric and sunphotometric observations, is also presented.

2. EXISTING METHODS

This study concentrates on methods that can produce both τ_a and β. The former coefficient has been in use at NREL for a long time, and new τ_a data can thus bring continuity with older datasets. The latter has a more physical basis and can be compared to, or validated against, independent sunphotometric measurements, as will be detailed in Section 4.

2.1 General concepts

Any radiation model that evaluates solar irradiance as a function of atmospheric information (including turbidity) can be used backwards to derive turbidity from irradiance measurements. In some cases, like with the Louche or METSTAT models, an analytic solution can be derived, using only algebraic manipulation. When using more elaborate models like CPCR2 [9] or REST2 [10], an iterative solution must be implemented. In essence, all radiation models used in backward mode are "implicit" turbidity models. In contrast, some explicit turbidity models have been devised, such as MLWT1 ([5] and MLWT2 [11]).

One general difficulty with the turbidity retrieval method scrutinized here is that clear conditions must exist, and therefore have to be isolated from all-sky data series, even in the absence of cloud information. More specifically, a clear line of sight (CLS) between the radiometer and a region of $\approx 3°$ around the sun is sufficient for the methods investigated here, since they use measurements of DNI only. A practical methodology to isolate CLS events *a posteriori* is presented in Section 3.

2.2 Modeling

The following seven radiation or turbidity models (listed in chronological order of publication) are tested here: Louche (Louche et al., 1987), CPCR2 [9], METSTAT [6, 7], MLWT1 [5], MLWT2 [11], REST [11], and REST2 [10]. The general principle behind the derivation of τ_a or β from DNI is directly linked to the main equation used by all broadband radiation models. The generic form of this equation always resembles that of the REST model, used here for identification purposes:

$$E_{bn} = E_{0n}T_aT_RT_gT_oT_nT_w \qquad (1)$$

where E_{bn} is the measured DNI, E_{0n} is the extraterrestrial irradiance for the time of measurement, and T_R, T_g, T_o, T_n, T_w, T_a are the transmittances of the individual extinction processes: Rayleigh scattering, mixed gases, ozone, nitrogen dioxide, water vapor and aerosols, respectively. Based on Bouguer-Lambert-Beer's law, the aerosol transmittance can be expressed as $\exp(-m_a\tau_a)$, where m_a is the aerosol optical mass. Therefore:

$$\tau_a = [\ln(T_RT_gT_oT_nT_w) - \ln(E_{bn}/E_{0n})]/m_a. \qquad (2)$$

Once τ_a is determined, it is possible to derive β. This is done analytically in the case of Louche, MLWT1, MLWT2 and REST because the function $\tau_a=f(\beta)$ in these models is simple enough, and thus can be reversed. CPCR2 and REST2 are two-band models with more sophistication, and thus require an iterative solution. METSTAT was not devised to provide β. For the present purpose, a simple workaround consists in scaling METSTAT's τ_a outputs by the ratio β/τ_a from MLWT1. To accelerate convergence, the latter model's results are also used here to provide the necessary seed input for CPCR2 and REST2 at each time step.

2.3 Default values

Some of the inputs to the models may not be measured at the radiometric sites where the method is to be applied. Even if normally measured, such data may be occasionally missing. Based on the error analysis in [11], the ozone amount (O3) and station pressure (Pr) can be considered second-order inputs because their impact on DNI is small. These variables are usually not measured at most sites anyway, thus a default value has generally to be used. Since this analysis targets the southwest US, a monthly climatology of O3 has been derived from ground measurements at regional sites belonging to the WOUDC network. In contrast, Pr is a strong function of elevation, which is always a known quantity. Hence, Pr can be evaluated, once at each site, with the method used in REST2 for convenience.

The amount of nitrogen dioxide (NO2) would only be of concern over polluted areas. In Denver, for instance, photochemical smog occasionally produces a lot of NO2, as signaled by the brownish color of the air during such episodes. Over remote areas and nearly all of the southwest US, the tropospheric NO2 contribution is virtually inexistent. This leaves only the stratospheric NO2 amount, which can be defaulted to a fixed value, 0.2 matm-cm. (NO2 is actually only considered by MLWT1, MLWT2, REST and REST2.)

Models such as MLWT1, MLWT2 or REST do not require α as an input because they implicitly default it to its conventional 1.3 value. In the case of Louche, CPCR2 and REST2, α is required, which creates a problem since it is an unknown. (α and β are two byproducts of AOD measurements, which are precisely missing here, by definition.) The effect of α on DNI is non-negligible, but significantly less than that of β [10]. The workaround used here is to consider a

local monthly climatology of α, obtained as an average of AERONET data at all existing sites in the southwest US. Note that the mean monthly α obtained here is generally not too different from 1.3 anyway. If the method was to be applied in regions with widely different aerosol regimes, such as maritime, desert or polluted urban areas, a larger departure from 1.3 would occur.

2.4 <u>Precipitable water</u>

Based on the discussion in [11] it is clear that a critical term on the right-hand side (RHS) of Eq. (2) is the water vapor transmittance, T_w, which is a direct function of PW. The latter has a strong spatial and temporal variability, but is usually not measured at radiometric sites, which creates difficulties in practice. Various strategies can be pursued:

• Use PW measurements from a nearby sunphotometric station, if close enough and over homogeneous terrain; such measurements normally exist at 15-min intervals, but with frequent missing periods. In practice, this avenue is of limited interest, since the main purpose of the turbidity method is to provide data at sites far away from sunphotometric stations. However, for validation purposes, this avenue is ideal (see Section 4).

• Use PW measurements from a nearby GPS station, if close enough and over homogeneous terrain; such measurements normally exist at 30-min intervals, day or night with no weather restrictions, and with only occasional missing data.

• Use reanalysis data; for instance, NASA's Modern-Era Retrospective analysis for Research and Applications (MERRA) provides gridded PW data at hourly intervals since 1979 (no missing data), with currently a 2/3° x 1/2° spatial resolution.

• Use spaceborne observations, from e.g., MODIS; the availability of data, their accuracy, as well as the spatial and temporal resolution, vary by satellite sensor.

• Use radiosonde data from a nearby station; the density of this network is now lower than that of GPS sites, and it reports at much less frequency too (12-hour vs. 30-min), hence this method is unlikely to be used in general.

• Use an empirical model relating PW to local measurements of temperature, T, and relative humidity, RH. Such data are normally available at radiometric sites, and at the same frequency as the radiation data (e.g., 1-min).

The latter avenue has been widely employed, particularly by NREL for the original NSRDB, when radiosonde data were used to derive a general empirical PW model for the whole US [12]. During the last decade, the density of the GPS network has increased dramatically over the US and many other countries. It is thus possible to either (i) interpolate GPS data over time and space; or (ii) use their PW, T and RH data to derive a locally calibrated empirical model. The first option presents the difficulties and risks associated with a double interpolation, both in space and time. Depending

on distance and topography, this procedure may return incorrect estimates of PW. It might thus be preferable to use PW, T and RH data from the closest GPS site, derive an empirical function PW=f(T, RH) based on all available GPS data, and then recalculate PW at the radiometric site based on the local T, RH data at that site. The various steps of this approach are detailed in what follows. The saturation pressure, e_s, is first calculated as a function of T [13]. The vapor pressure, e_v, is then obtained as the product $e_s \cdot$RH. Finally, a least-squares method is used to fit the PW data to some simple function of e_v. A linear function is usually sufficiently good, but a more sophisticated function:

$$PW = a + b\,e_v^{\,c} \tag{3}$$

may be slightly better.

A first example of the relationship between the observed PW and e_v data is shown in Fig. 1 for the DSRC GPS site in Boulder, CO, using 30-min data over the period 2001–2012. The best fit is obtained with Eq. (3) and $a = -0.03368$, $b = 0.22344$ and $c = 0.92833$ (R = 0.912). At NREL's Solar Radiation Research Lab (SRRL) in Golden, CO, reliable GPS-PW data started on Aug. 30, 2012, so that only about 5 months of data were available as of this writing. This limitation (particularly in the case of large PW values, see Fig. 1), in addition to the distance ($\approx$28 km) and topographic features between Boulder and Golden, may explain the different coefficients obtained there: $a = -0.13232$, $b = 0.27932$ and $c = 0.83243$ (R = 0.898). The large scatter of the data points is a usual characteristic of this type of empirical model, conducive to significant RMS errors, up to $\pm$30–50%, depending on site.
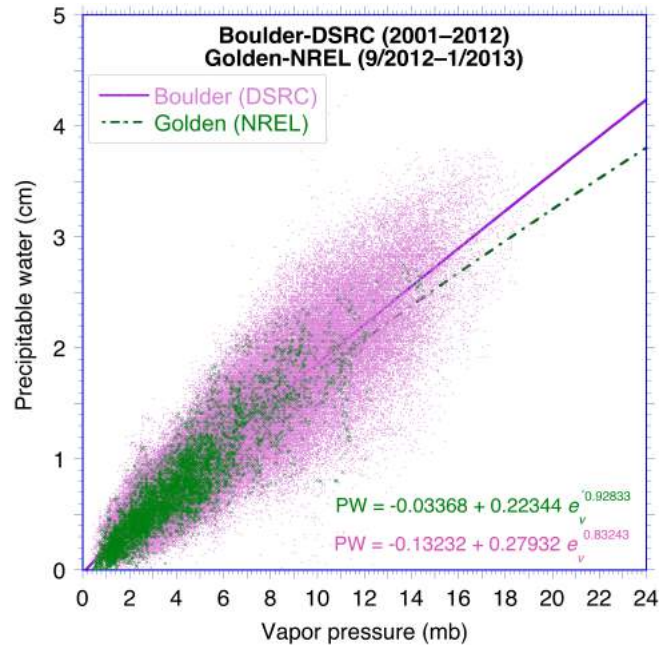

Fig. 1: Relationship between PW and e_v at two GPS sites.

Figure 2 compares the current GPS-PW data at SRRL to three other sources of data: the 940-nm channel of a collocated Prede POM-01 sunphotometer; the 1-min empirically fitted PW from the local T and RH; as well as the MERRA reanalysis for the local grid box. Both the 30-min GPS and 60-min MERRA data were interpolated to the same 1-min time step as the radiometric and meteorological data. For MERRA, a narrow domain was defined between longitudes 104.95° and 105.45° West, so as to avoid most high-elevation areas west of SRRL (longitude 105.18° W). Still, the MERRA PW data are grid-box averages and appear too low compared to SRRL's GPS data. The scatter in the MERRA data is much less than that of the empirical fit, however. In contrast, the sunphotometer data is much too inaccurate for consideration: the instrument was not calibrated correctly (and still not is, as of this writing), and the cloudy periods were not filtered out.
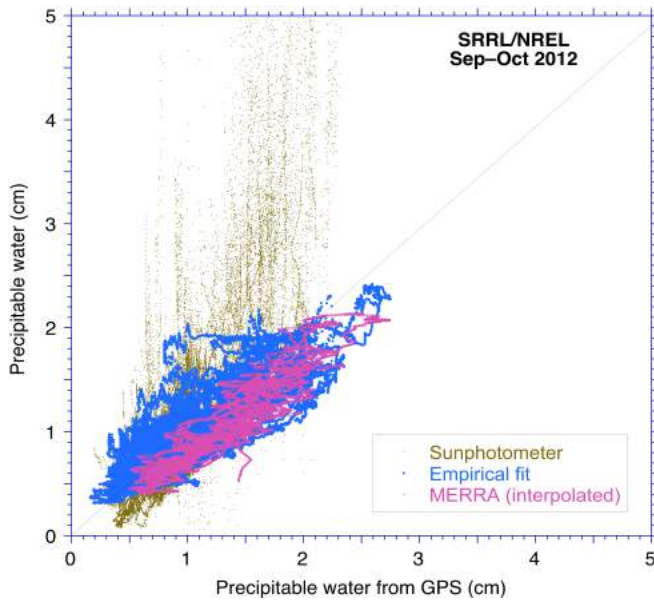

Fig. 2: Determination of 1-min precipitable water by four methods at NREL's SRRL site in Golden, CO.

Figure 3 shows a comparison between the PW data provided by the AERONET sunphotometer at the BSRN-Boulder station and the data obtained from the empirical f(T, RH) model of Eq. (3), using BSRN's T and RH data and coefficients determined at the GPS-DSRC site, ≈23 km west of the BSRN station. In addition to the typical scatter introduced by the empirical model, an unexpected bias is also apparent. It may be due to a strong topographic effect, since DSRC is located on the foothills of the Rocky Mountains and at a slightly different elevation (1670 m) compared to the BSRN site (1604 m).

From the discussion above, and similar results at other locations (not shown for conciseness), it is clear that the uncertainty in PW can be substantial, unless it is measured onsite with a GPS device or a well-calibrated sunphotometer. The

tabulations in [5] provide actual results of a detailed error analysis, showing the propagation of errors in PW, O3, NO2 and DNI into τ_a.
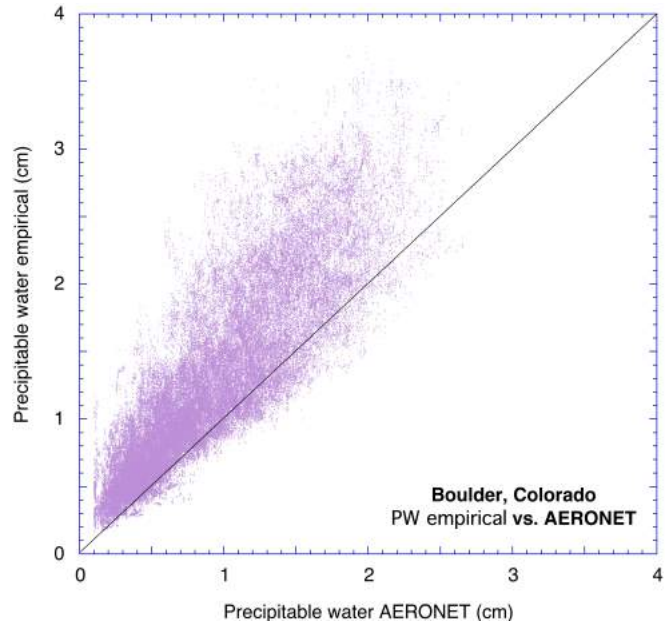

Fig. 3: Empirical determination of precipitable water vs. reference AERONET sunphotometer data for Boulder, CO.

3. CLOUD FILTERING

The CLS condition referred to above is critical for the success of the turbidity method, such that each DNI data point used as input to the model represents clear-sky conditions within the field of view of the radiometer. Two avenues can be considered to eliminate cloud artifacts and precisely discriminate CLS conditions:

• Filter out cloud conditions in the DNI data, and use all the remaining (CLS) data to evaluate τ_a and/or β.

• Use all DNI data, and eliminate those τ_a or β data points that cannot physically relate to CLS conditions.

The first approach can be implemented with the Long filter [14]. The Fortran files and executables of the Long algorithm (as provided by its author) have been found slow and cumbersome to use. Hence, the second approach has been developed, inspired by the cloud-screening method that was adopted by AERONET to provide reliable AOD data from sunphotometric observations [15]. Since the retrieved τ_a and β are extremely sensitive to changes in DNI, the pattern of their short-term variations over time indicates possible cloud interference. The method has been developed and tuned here for 1-min DNI data, but could be adjusted to accommodate shorter or longer time steps. The approach consists of a series of tests that are applied to consecutive 1-min retrievals of τ_a, as determined with the REST2 model. A sequence of 7

consecutive data points over a period of ±3 minutes is defined for each (central) data point. A suite of stability tests is applied on this 6-min period to decide whether it can be considered CLS:

(i) The 6-min period is eliminated if it contains missing or unfitting DNI data. Each DNI data point must be at least 120 W/m^2, and its zenith angle, Z, must be less than 85°. These requirements remove data points directly affected by passages of thick clouds or low-sun issues.

(ii) Whereas, under clear and stable conditions, DNI varies smoothly during the day because it depends on Z, τ_a is nearly independent of it [5], and is therefore relatively constant. Additionally, the aerosol load does not normally vary fast under natural conditions (but exceptions do exist, as discussed in Section 4), so that it should remain roughly constant over short time intervals. Each 1-min transition of the 6-min period is thus scrutinized. The relative change is compared to a threshold limit that is defined as a decreasing function of τ_a. A small relative change in the case of a large τ_a is as important as a large change in the case of a small τ_a, because both cases actually correspond to similar relative changes in DNI.

(iii) The 6-min mean absolute variation should be small enough. The period is rejected if the RMS sum of all 6 absolute variations in larger than a specified limit.

(iv) The mean second derivative of τ_a vs. time should be small enough [15].

(v) The retrieved β should be plausible. To avoid false cloud diagnostics, retrieved β values below 0.025 are considered valid. Moreover, REST2's β predictions below 0.005 are floored to that value.

4. VALIDATION

To validate the method and select the best radiation model(s) for the most accurate retrieval of β or τ_a, 9 years (2001–2009) of irradiance data from the BSRN station in Boulder are used. A collocated AERONET sunphotometer provides AOD at various wavelengths, out of which α and β are derived by fitting the AOD data to the linearized Ångström equation [10, 16].

4.1 Potential sources of uncertainty

The total uncertainty in τ_a can conceptually be evaluated from Eq. (2). Three distinct sources of error are involved: (1) intrinsic modeling errors in the actual determination of the individual transmittances—in the left block of Eq. (2)'s RHS—if ideally perfect inputs are assumed; (2) errors in the atmospheric inputs necessary to calculate these transmittances; and (3) experimental errors in DNI.

Errors of the first kind can be inferred from those related to the more usual task of determining DNI from AOD. For instance, recent validation studies (e.g., [11, 16]) have eval-

uated the performance of the 7 models mentioned above, when high-quality inputs (such as AOD and PW) are used to calculate DNI. Since AOD is the major factor affecting DNI under cloudless conditions, a comparatively similar level of performance likely exists when these models are rather used backwards. However, for the present inverse problem, the determination of β depends on α, which is not known *a priori*. The modeling performance is thus not purely intrinsic in this case, but incorporates the propagation of errors caused by an uncertain α. Errors of the second kind are dominated by those in PW. To evaluate β from τ_a, additional errors are introduced by the uncertain nature of α, since it is normally not measured locally. Finally, the experimental errors are directly related to the quality and type of equipment and the frequency of experimental problems.

4.2 Validation for Boulder, Colorado

At BSRN-Boulder, DNI is measured with an Eppley NIP pyrheliometer. The global and diffuse components are measured with Eppley PSP pyranometers. All these instruments are well characterized. BSRN data must pass a detailed control procedure. Still, it is instructive to check if the three independently measured components actually achieve closure. The closure error (CE) is defined here as:

$$CE = (E_{bn} \cos Z + E_d) / E - 1 \qquad (4)$$

where E_d and E are the diffuse and global components, respectively. At a high-quality research station like those of BSRN—where radiometers are well calibrated, regularly cleaned and maintained—CE remains normally close to 0 for $Z < 85°$, as it should. Malfunctions in at least one of the three radiometers do occur occasionally, however, making time series of CE a good diagnostic tool. Negative values below a few percent tend to indicate a loss of pyrheliometer signal, usually due to misalignment or tracker issues. Based on an analysis of error propagation between β and DNI [1], it is estimated that a loss of signal of –3% corresponds to a possible maximum absolute error of +0.03 in β, which can lead to seriously incorrect results under low-turbidity conditions. Therefore, only data points with CE > –3% have been considered in what follows.

The strong effect of any bias in DNI measurement, most importantly over low-turbidity areas, makes the correct calibration of pyrheliometers, as well as their regular cleaning and maintenance, an essential condition of success. The use of photodiode instruments, such as rotating shadowband radiometers, may introduce additional uncertainty because they cannot be completely corrected for spectral and air-mass effects or cosine errors, and because basic quality control through the use of Eq. (4) is not possible in their case, since DNI is not obtained independently, but by difference between the global and diffuse components. For NREL SOLRMAP stations, the latter shortcoming is partially overcome through a redundant global sensor used primarily to provide an independent value for E in Eq. (4).

The AERONET station started operation at the BSRN-Boulder site in May 2001. Three periods with anomalous data have been identified, when α was much higher than its normal maximum of ≈2.0, yielding anomalously low values of β. Most likely, at least one sunphotometer channel was miscalibrated or defective during those periods, but this problem was surprisingly not caught during the QC procedure established by AERONET as part of its routine analysis that brings the raw data (Level 1) to the highest degree of quality (Level 2), which is used here. These periods have been eliminated to guarantee consistent validation results.

PW can be obtained locally from the AERONET sunphotometer at the same time as AOD. This is considered the best method for validation purposes. However, to test how suboptimal PW data can affect the AOD results (since this would correspond to most situations in practice), an alternate determination of PW is possible, using Eq. (3) with local values of e_v and empirical coefficients determined from the DSRC GPS site (Figs. 1 and 3).

The 9-year validation period originally contained nearly 2 million data points of 1-min sunup DNI, T and RH from BSRN-Boulder. After elimination of all questionable data points, and elimination of all valid (i.e., cloud-free) results whose time stamps were more than ±1.5 minute away from any valid AERONET reference data point, the final validation dataset consisted of 113,934 points. Summary statistical results obtained with the different models mentioned in Section 2 are compiled in Table 1, for both the optimal PW inputs (from the local sunphotometer) and the suboptimal case (using the empirical PW model). This validation is done with reference to β only, since τ_a cannot be measured directly, and is thus affected by the imperfect values of α used as input at each time step.

Figure 4 shows diurnal variations of the REST2-modeled β and AERONET-derived β for a 6-day period in June 2002, when the DNI trace indicates successions of clear and cloudy situations, under relatively low-AOD conditions for the season, with however some instability around noon. The modeled and experimental β vales agree generally well, with occasional significant differences, caused by a much different α than assumed. This plot also reveals that the cloud-screening method of Section 3 errs on the conservative side: some valid AOD data points are rejected during mid-day periods, because of rapid fluctuations in the DNI signal (possibly caused by a thin layer of smoke; see below). This should not be a big problem in practice, since the method is aimed at sunny regions, where it is better to be on the conservative side (with some occasional false positives) since the inclusion of cloud-contaminated data could result in serious AOD overestimation.

A similar plot, but for a 3-day period two weeks later (Fig. 5) exemplifies the case of very hazy and unstable conditions, during which AOD reached the maximum value of the whole 9-year dataset. The underlying episode of thick

smoke was caused by the Hayman Fire—the largest forest fire in Colorado's history. From June 8 to July 2, it burned a 560-km^2 area located ≈110 km south of Boulder. Interestingly, many of the data points passed the cloud-screening algorithm, and matched the AERONET data relatively well, in spite of the unusual conditions. The peak β values observed on July 2 created a strong attenuation in DNI, similar to what a cirrus cloud would have produced, for instance.

TABLE 1. SUMMARY STATISTICS FOR THE METHOD'S VALIDATION AT TWO SITES

| Station	Meas.	REST2	CPCR2	MLWT1	MLWT2	REST	Louche	METSTAT
Boulder 2001–2009, PW from AERONET								
N	113934							
Mean	0.039	0.037	0.037	0.050	0.043	0.042	0.046	0.043
Min	0.001	0.007	0.008	0.008	0.005	0.005	0.001	0.001
Max	0.758	0.728	0.500	0.820	0.762	0.635	1.012	0.789
MBD	—	-0.002	-0.002	0.011	0.004	0.003	0.008	0.004
RMSD	—	0.012	0.013	0.016	0.012	0.012	0.017	0.013
Boulder 2001–2009, PW = f(T,RH)								
N	113934							
Mean	0.039	0.032	0.033	0.044	0.037	0.038	0.043	0.039
Min	0.001	0.005	0.005	0.005	0.005	0.005	0.001	0.001
Max	0.758	0.709	0.500	0.791	0.746	0.626	0.994	0.765
MBD	—	-0.007	-0.006	0.005	-0.002	-0.001	0.004	0.000
RMSD	—	0.014	0.015	0.014	0.013	0.012	0.016	0.014
Tucson 2010–2011, w from AERONET								
N	14364							
Mean	0.013	0.019	0.019	0.030	0.024	0.024	0.025	0.025
Min	0.004	0.009	0.010	0.018	0.012	0.013	0.010	0.013
Max	0.086	0.067	0.066	0.076	0.068	0.065	0.079	0.078
MBD	—	0.005	0.006	0.017	0.011	0.011	0.012	0.012
RMSD	—	0.008	0.009	0.018	0.012	0.012	0.013	0.013
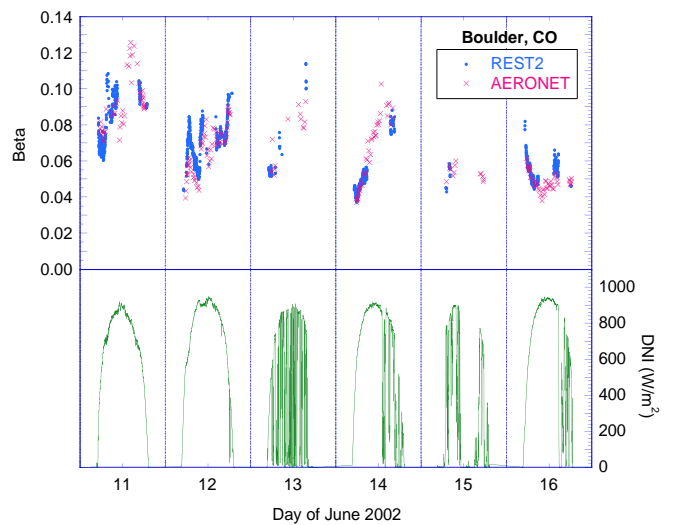
Fig. 4: Diurnal variations of the modeled and measured values of β (top) and DNI (bottom) at Boulder, June 2002.

4.3 Validation for Tucson, Arizona

A similar study as in Section 4.2 can be conducted at the University of Arizona in Tucson, where an AERONET station operated until January 2011, and an NREL SOLRMAP radiometric station has been operating since November 2010. The 3-month common period is much shorter than the Boulder test period, and is limited to the winter season, during which AOD is at its lowest point of the year. Moreover, T and RH were missing during that period, so that only the sunphotometric PW data can be used here. The cumulative statistics that appear in Table 1 tend to confirm what was found for Boulder, with however a comparatively larger difference between the results from the best models (REST2 and CPCR2) and those from the other models.
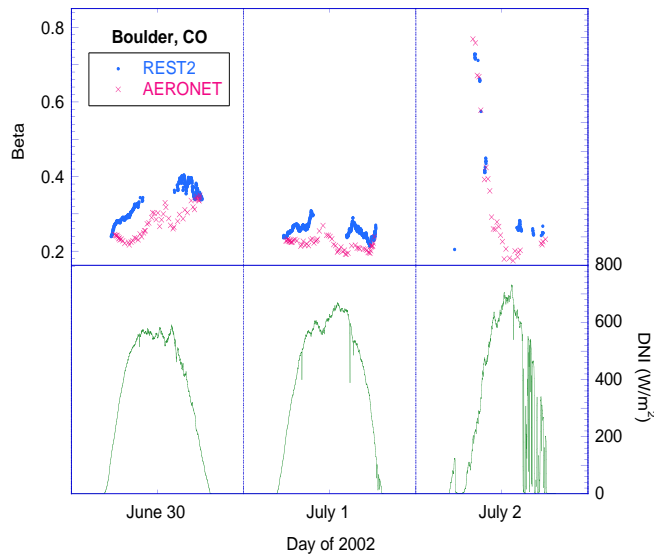
Fig. 5: Diurnal variations of the modeled and measured values of β (top) and DNI (bottom) at Boulder, during a strong haze episode caused by the Hayman Fire.

A scatterplot of the results obtained with REST2 for both Tucson and Boulder appears in Fig. 6. The scatter along the diagonal results from the various sources of error discussed above, particularly those in α and in the observed E_{bn} and PW. Two series of data points deserve more scrutiny. The orange rectangle delimits the largest values of β obtained during July 2, 2002, at the peak of the Hayman Fire episode over Boulder. The green circle contains outliers obtained on July 20, 2005, for which the only reasonable explanation would be the adverse effect of an extremely high α.

4.4 Practical applications

In practice, the error propagation from experimental errors in E_{bn}, or from biases in α or PW, to τ_a and β may be significant, as discussed above. This results in noticeable scatter on an hourly or daily basis, as shown in Fig. 6. Nevertheless, these errors mostly cancel out when evaluating month-

ly averages, which is confirmed by the very low MBD statistics in Table 1. Therefore, the retrieved monthly-average β (or τ_a) should always be accurate enough for its intended application. Based on the preliminary results presented here, it is estimated that the uncertainty in the *monthly-average β* is ≈0.012, in the favorable case that the monthly bias in DNI or PW is close to 0. In comparison, the uncertainty in *instantaneous* AOD data from AERONET is ≈0.010 [17].
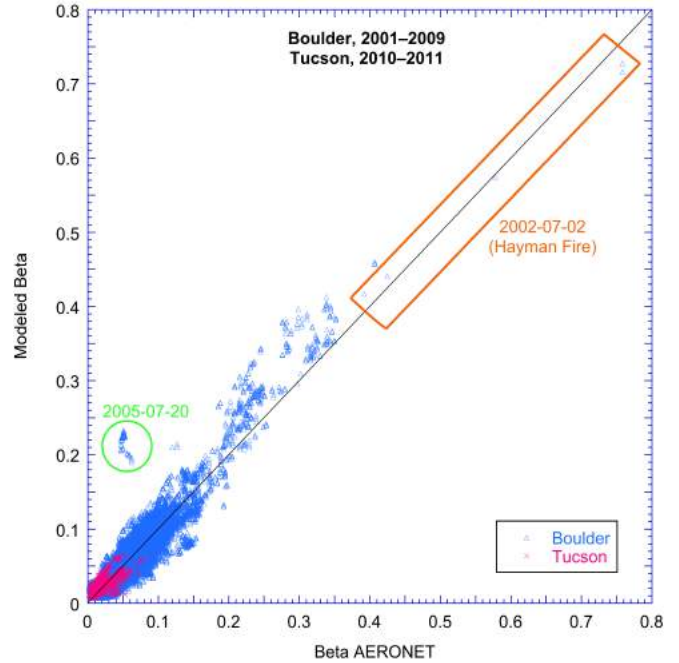
Fig. 6: Scatterplot of modeled vs. measured values of β at Boulder and Tucson.

5. CONCLUSION

This investigation has provided a complete method to evaluate two measures of turbidity (τ_a and β) using regular broadband measurements of DNI. This method is possible because of the high sensitivity of DNI on turbidity. However, compared to the usual method of deriving AOD from sunphotometric data, the "DNI turbidity method" described here must deal with some critical difficulties: (i) selection of an appropriate radiative model; (ii) critical need for accurate simultaneous PW data; (iii) dependence on an effective cloud screening procedure; (iv adverse effects of the DNI measurement uncertainty; and (v) need for a preliminary estimate of α so that β can be derived from τ_a.

Practical solutions are presented here to iron out all these difficulties. An extensive validation carried out with collocated radiometric/sunphotometric data from Boulder and Tucson shows that the REST2 radiative model normally delivers the best performance. Various experimental difficulties and sources of error associated with such a validation exercise are also discussed.

An original cloud screening algorithm has been specially developed, using a similar principle as that of AERONET. It is currently tuned for 1-min data, which is the normal reporting frequency at most NREL-sponsored radiometric stations. This algorithm uses contiguous 6-min τ_a data packets and evaluates their internal smoothness to detect cloud contamination. The present results indicate that this screening is very effective, albeit possibly too stringent, and well adapted to the case of low-cloudiness areas envisioned here.

Assuming an efficient cloud screening and unbiased DNI data, the main sources of uncertainty are in the PW input and in the assumed α values. Considering that the effect of instantaneous errors in α can be high on hourly or daily time scales, the method should target the development of *monthly* β datasets. It is anticipated that the determination of hourly or daily time series of τ_a can be done accurately enough, but this cannot be verified easily, and limits the application of the retrieved data to only those radiation models using τ_a rather than a spectral AOD input, such as β.

While low-uncertainty daily or hourly aerosol estimates would contribute to even greater accuracy in solar modeling than just monthly averages, the effort to produce a geographically broad aerosol dataset is of a much greater magnitude. The procedure described here, if advanced with input data of sufficient quality, should represent a significant improvement over previous climatological aerosol data sets. It is estimated that, for the southwest US, the resulting monthly uncertainty in β should be better than 0.012, assuming unbiased data of PW and DNI can be obtained. The uncertainty in τ_a should even be lower. Future work should include the validation of the method at stations obtaining DNI from photodiode radiometers, and the use of the retrieved turbidity data to improve gridded AOD datasets derived from satellite observations, particularly over the southwest US.

6. ACKNOWLEDGMENTS

7. REFERENCES

1. Gueymard C.A., Temporal variability in direct and global irradiance at various time scales as affected by aerosols. *Solar Energy*. **86**: 3544-2553, 2012.
2. Ruiz-Arias J.A. *et al.*, Assessment of the Level-3 MODIS daily aerosol optical depth in the context of surface solar radiation and numerical weather modeling. *Atmos. Chem. Phys.* **13**: 675-692, 2013.
3. Wilcox S.M. and Myers D., Joint solar power industry and Department of Energy Solar Resource and Meteorological Assessment Project (SOLRMAP). Proc. *Optical Modeling and Measurements for Solar Energy Systems III, vol. 7410*. San Diego, CA, SPIE, 2010.
4. Wilcox S. and McCormack P., Implementing Best Practices for Data Quality Assessment of the National Renewable Energy Laboratory's Solar Resource and Meteorological Assessment Project. Proc. *Solar 2011 Conf.* Raleigh, NC, ASES, 2011.
5. Gueymard C.A., Turbidity determination from broadband irradiance measurements: A detailed multi-coefficient approach. *J. Appl. Meteorol.* **37**: 414-435, 1998.
6. Maxwell E.L., METSTAT—The solar radiation model used in the production of the National Solar Radiation Data Base (NSRDB). *Solar Energy*. **62**: 263-279, 1998.
7. Maxwell E.L. and Myers D.R., Daily estimates of aerosol optical depth for solar radiation models. Proc. *Solar '92, Annual ASES Conf.,* Cocoa Beach, FL, 1992.
8. Louche A. *et al.*, Determination of Angström's turbidity coefficient from direct total solar irradiance measurements. *Solar Energy*. **38**: 89-96, 1987.
9. Gueymard C.A., A two-band model for the calculation of clear sky solar irradiance, illuminance, and photosynthetically active radiation at the Earth's surface. *Solar Energy*. **43**: 253-265, 1989.
10. Gueymard C.A., REST2: High performance solar radiation model for cloudless-sky irradiance, illuminance and photosynthetically active radiation—Validation with a benchmark dataset. *Solar Energy*. **82**: 272-285, 2008.
11. Gueymard C.A., Direct solar transmittance and irradiance predictions with broadband models. *Solar Energy*. **74**: 355-395, 2003.
12. Myers D.R. and Maxwell E.L., Hourly estimates of precipitable water for solar radiation models. Proc. *Solar '92, Annual ASES Conf.,* Cocoa Beach, FL, 1992.
13. Gueymard C.A., Assessment of the accuracy and computing speed of simplified saturation vapor equations using a new reference data set. *J. Appl. Meteorol.* **32**: 1294-1300, 1993.
14. Long C.N., The Shortwave (SW) Clear-Sky Detection and Fitting Algorithm: Algorithm Operational Details and Explanations, Rep. ARM TR-004, Atmospheric Radiation Measurement Program, DOE, 2000.
15. Smirnov A. *et al.*, Cloud screening and quality control algorithms for the AERONET database. *Remote Sens. Environ.* **73**: 337-349, 2000.
16. Gueymard C.A., Clear-sky irradiance predictions for solar resource mapping and large-scale applications: Improved validation methodology and detailed performance analysis of 18 broadband radiative models. *Solar Energy*. **86**: 2145-2169, 2012.
17. Holben B.N. *et al.*, AERONET—A federated instrument network and data archive for aerosol characterization. *Remote Sens. Environ.* **66**: 1-16, 1998.